Evaluating properties of environmental contours

Arne B. Huseby
University of Oslo, Norway

Erik Vanem
DNV - GL, Norway

Karoline Eskeland
University of Oslo, Norway

Environmental contours are widely used as a basis for e.g., ship design. The traditional approach to environmental contours is based on the well-known Rosenblatt transformation. However, due to the effects of this transformation the probabilistic properties of the resulting environmental contour can be difficult to interpret. An alternative approach to environmental contours uses Monte Carlo simulations on the joint environmental model, and thus obtain a contour without the need for the Rosenblatt transformation. This contour have well-defined probabilistic properties, but may sometimes be overly conservative in certain areas. In this paper we give a precise definition of the concept of exceedence probability which is valid for all types of environmental contours. Moreover, we show how to estimate the exceedence probability of a given environmental contour, and use this to compare different approaches to contour construction. The methods are illustrated by numerical examples based on real-life data.

1 INTRODUCTION

Environmental contours are widely used as a basis for e.g., ship design. Such contours allow the designer to verify that a given mechanical structure is safe, i.e, that the failure probability is below a certain value. A realistic model of the environmental loads and the resulting response is crucial for structural reliability analysis of mechanical constructions exposed to environmental forces. See (Winterstein et al. 1993) and (Haver & Winterstein 2009). For applications of environmental contours in marine structural design, see e.g., (Baarholm et al. 2010), (Fontaine et al. 2013), (Jonathan et al. 2011), (Moan 2009) and (Ditlevsen 2002).

The traditional approach to environmental contours is based on the well-known *Rosenblatt transformation* introduced in (Rosenblatt 1952). This transformation maps the the environmental variables into independent standard normal variables. Using the transformed environmental variables a contour with the desired properties can easily be constructed by identifying a sphere centered in the origin and with a suitable radius. More specifically, the sphere can be chosen so that any non-overlapping convex failure region has a probability less than or equal to a desired exceedence probability. The corresponding environmental contour in the original space can then be found by transforming the sphere back into the original space.

However, a convex region in the transformed space does not necessarily correspond to a convex region in the original space. Thus, the properties of the resulting environmental contour are difficult to interpret. To avoid such problems, contours in the original space can be constructed by using Monte Carlo simulations on the joint environmental model. See (Huseby et al. 2013), (Huseby et al. 2015a) and (Huseby et al. 2015b). By using this methodology, every calculation is carried out in the original environmental space, and thus the use of the Rosenblatt transformation is avoided. Contours constructed using the suggested Monte Carlo simulation approach will always be convex sets. This yields a more straightforward interpretation of the contours. Another advantage of this approach is a more flexible framework for establishing environmental contours, which for example simplifies the inclusion of effects such as future projections of the wave climate related to climatic change. See (Vanem & Bitner-Gregersen 2012). It should be noted, however, that convex contours may not fit the joint distribution of the environmental variables well. Thus, this limitation may sometimes be too restrictive.

In this paper we give a precise definition of the concept of exceedence probability which is valid for all types of environmental contours. Moreover, we show how to estimate the exceedence probability of a given environmental contour, and use this to compare different approaches to contour construction. The methods are illustrated using the examples introduced in (Vanem & Bitner-Gregersen 2015).

2 BASIC CONCEPTS AND RESULTS

In this paper we consider cases where the environmental conditions can be described by a vector $(T, H) \in \mathbb{R}^2$. An *environmental contour* is then defined as the boundary of a set $\mathcal{B} \subseteq \mathbb{R}^2$, and denoted $\partial\mathcal{B}$.

A given mechanical structure can withstand environmental stress up to a certain level. The *failure region* of the structure is the set of states of the environmental variables that imply that the structure fails. The exact shape of the failure region of a structure may be unknown. Still it may be possible to argue that the failure region belongs to a certain family which we denote by $\mathcal{E}$. A given environmental contour $\partial\mathcal{B}$ will be evaluated with respect to this family. The family $\mathcal{E}$ is chosen relative to $\mathcal{B}$ in such a way that $\mathcal{F} \cap \mathcal{B} \subseteq \partial\mathcal{B}$ for all $\mathcal{F} \in \mathcal{E}$. Thus, a failure region $\mathcal{F}$ may intersect with the boundary of $\mathcal{B}$ but not the interior of $\mathcal{B}$. The *exceedence probability* of $\mathcal{B}$ with respect to $\mathcal{E}$ is defined as:

$$P_e(\mathcal{B}, \mathcal{E}) = \sup\{P[(T, H) \in \mathcal{F}] : \mathcal{F} \in \mathcal{E}\}.$$

We observe that the exceedence probability defined above represents an upper bound on the failure probability of the structure assuming that the true failure region is a member of the family $\mathcal{E}$. Of particular interest are cases where one can argue that the failure region of a structure is *convex*. That is, cases where $\mathcal{E}$ is the class of all convex sets which do not intersect with the interior of $\mathcal{B}$. We denote the interior of $\mathcal{B}$ by $\mathcal{B}_o$.

2.1 *Maximal failure regions*

A failure region $\mathcal{F} \in \mathcal{E}$ is said to be *maximal* if there does not exist a region $\mathcal{F}' \in \mathcal{E}$ such that $\mathcal{F} \subset \mathcal{F}'$. The family of maximal regions in $\mathcal{E}$ is denoted by $\mathcal{E}^*$. If $\mathcal{F}_1, \mathcal{F}_2 \in \mathcal{E}$ and $\mathcal{F}_1 \subseteq \mathcal{F}_2$, we obviously have:

$$P[(T, H) \in \mathcal{F}_1] \leq P[(T, H) \in \mathcal{F}_2].$$

From this it follows that:

$$P_e(\mathcal{B}, \mathcal{E}) = \sup\{P[(T, H) \in \mathcal{F}] : \mathcal{F} \in \mathcal{E}^*\}.$$

This simple observation sometimes simplifies the calculation of $P_e(\mathcal{B}, \mathcal{E})$.

In order to explain this in further detail, we need the concept of a *supporting hyperplane* of a set. If Π is a hyperplane in $\mathbb{R}^n$, we let Π^- and Π^+ denote the two half-spaces bounded by the hyperplane Π. In general a supporting hyperplane of a set $\mathcal{S} \in \mathbb{R}^n$, is a hyperplane Π such that we either have $\mathcal{S} \subseteq \Pi^-$ or $\mathcal{S} \subseteq \Pi^+$, and such that $\mathcal{S} \cap \Pi \neq \emptyset$. In particular, if $\mathcal{S} \subseteq \Pi^-$, we say that Π^+ is a *supporting half-space* of $\mathcal{S}$. We observe that if Π^+ is a supporting half-space of $\mathcal{S}$, we have that $\Pi^+ \cap S \subseteq \partial\mathcal{S}$.

We then consider a case where the set $\mathcal{B}$ is convex, where all sets in the family $\mathcal{E}$ are convex as well, and let $\mathcal{F} \in \mathcal{E}$. Then it follows by standard convexity theory, that there exists a supporting hyperplane Π of $\mathcal{B}$ such that $\mathcal{B} \subseteq \Pi^-$ and $\mathcal{F} \subseteq \Pi^+$. Moreover, since $\Pi^+ \cap \mathcal{B} \subseteq \partial\mathcal{B}$, and since every half-space is convex, it follows by the definition of $\mathcal{E}$ that $\Pi^+ \in \mathcal{E}$.

Assume then that $\mathcal{F} \in \mathcal{E}^*$. If this is the case, we cannot have $\mathcal{F} \subset \Pi^+$. Hence, the only possibility is that $\mathcal{F} = \Pi^+$. Thus, we have shown that every maximal failure region $\mathcal{F}$ is a supporting half-space of $\mathcal{B}$. Conversely, we have that if Π^+ is a supporting halfspace of $\mathcal{B}$, then we cannot find another supporting half-space Π'^+ such that $\Pi^+ \subset \Pi'^+$. Hence, if Π^+ is a supporting half-space of $\mathcal{B}$, then $\Pi^+ \in \mathcal{E}^*$.

We let $\mathcal{P}(\mathcal{B})$ denote the family of supporting half-spaces of $\mathcal{B}$. Then we may summarize the above discussion as follows:

Proposition 2.1 *Assume that $\mathcal{B}$ is convex and that $\mathcal{E}$ is a family of convex sets such that $\mathcal{F} \cap \mathcal{B} \subseteq \partial\mathcal{B}$ for all $\mathcal{F} \in \mathcal{E}$. Then $\mathcal{E}^* = \mathcal{P}(\mathcal{B})$. Moreover, we have:*

$$P_e(\mathcal{B}, \mathcal{E}) = \sup\{P[(T, H) \in \Pi^+] : \Pi^+ \in \mathcal{P}(\mathcal{B})\}.$$

2.2 *Transformed contours*

In this subsection we review the traditional aproach to environmental contours based on the well-known Rosenblatt transformation in the context of an exceedence probability defined relative to a family of failure regions. The Rosenblatt transformation, denoted Ψ, is such that if $(T', H') = \Psi(T, H)$, then T' and H' are independent standard normally distributed. See (Winterstein et al. 1993).

The contour for the transformed vector (T', H') is constructed as follows: Let $P_e < 0.5$ be the desired exceedence probability, and let $r > 0$ denote the $(1 - P_e)$-percentile in the standard normal distribution. We then introduce the set $\mathcal{B}'$, a circle centered at the origin and with radius r, and let $\mathcal{E}'$ be the family of all convex sets $\mathcal{F}'$ such that $\mathcal{F}' \cap \mathcal{B}' \subseteq \partial\mathcal{B}'$. By Proposition 2.1, we then have that $\mathcal{E}'^* = \mathcal{P}(\mathcal{B}')$. We then choose an arbitrary half-space $\Pi^+ \in \mathcal{P}(\mathcal{B}')$. By the rotational symmetry property of the bivariate normal distribution of (T', H') it follows that:

$$P[(T', H') \in \Pi^+] = P[T' > r] = P_e.$$

Since this is true for all $\Pi^+ \in \mathcal{P}(\mathcal{B}')$, we then get:

$$P_e(\mathcal{B}', \mathcal{E}') = \sup\{P[(T', H') \in \Pi^+] : \Pi^+ \in \mathcal{P}(\mathcal{B}')\} = P_e.$$

We then let $\mathcal{B} = \Psi^{-1}(\mathcal{B}')$, and let $\mathcal{E}$ be given by:

$$\mathcal{E} = \{\mathcal{F} = \Psi^{-1}(\mathcal{F}') : \mathcal{F}' \in \mathcal{E}'\},$$

where Ψ^{-1} denotes the inverse Rosenblatt transformation, and the inverse mapping $\Psi^{-1}(\mathcal{M})$ of an arbitrary set $\mathcal{M}$ is defined by

$$\Psi^{-1}(\mathcal{M}) = \{(t, h) = \Psi^{-1}(t', h') : (t', h') \in \mathcal{M}\}.$$

We then get that:

$$\begin{aligned} P_e(\mathcal{B}, \mathcal{E}) &= \sup\{P[(T, H) \in \mathcal{F}] : \mathcal{F} \in \mathcal{E}\} \\ &= \sup\{P[(T, H) \in \Psi^{-1}(\mathcal{F}')] : \mathcal{F}' \in \mathcal{E}'\} \\ &= \sup\{P[(T', H') \in \mathcal{F}'] : \mathcal{F}' \in \mathcal{E}'\} \\ &= \sup\{P[(T', H') \in \Pi^+] : \Pi^+ \in \mathcal{P}(\mathcal{B}')\} = P_e. \end{aligned}$$

Thus, the contour $\partial\mathcal{B}$ has the desired exceedence probability with respect to the family $\mathcal{E}$ of failure regions.

The problem with this approach is that since $\mathcal{E}$ consists of transformed convex sets, where the transformation depends on the joint distribution of (T, H), it may be difficult to argue that a given mechanical construction should have a failure region which belongs to this particular family. In order to do so we must argue that if $\mathcal{F}$ is the true failure region for the given mechanical construction, then $\Psi(\mathcal{F})$ must be convex. It is typically much easier to argue that the true failure region $\mathcal{F}$ itself is convex, and hence avoid an argument involving the joint distribution of the environmental variables. In order to accomplish this, however, the family $\mathcal{E}$ must be redefined, and hence the exceedence probability may change.

2.3 *Convex contours*

In (Huseby et al. 2013), (Huseby et al. 2015a) and (Huseby et al. 2015b) the focus was restricted to contours where the set $\mathcal{B}$ itself was *convex*. Moreover, the family $\mathcal{E}$ was chosen relative to $\mathcal{B}$ as the family of all convex failure regions $\mathcal{F} \subseteq \mathbb{R}^2$ such that $\mathcal{F} \cap \mathcal{B} \subseteq \partial\mathcal{B}$. By Proposition 2.1 this makes the calculation of the exceedence probability relatively simple.

In order to briefly explain the approach we let $P_e < 0.5$ be the desired exceedence probability of $\mathcal{B}$ with resepect to $\mathcal{E}$. In order to determine $\mathcal{B}$ such that $P_e(\mathcal{B}, \mathcal{E}) = P_e$, we start out by introducing the function $C(\theta)$ defined for $\theta \in [0, 2\pi)$ as:

$$C(\theta) = \inf\{C : P[T\cos(\theta) + H\sin(\theta) > C] = P_e\}.$$

This means that $C(\theta)$ is the $(1 - P_e)$-percentile of the distribution of $Y(\theta) = T\cos(\theta) + H\sin(\theta)$. Furthermore, we introduce for $\theta \in [0, 2\pi)$:

$$\Pi(\theta) = \{(t, h) : t\cos(\theta) + h\sin(\theta) = C(\theta)\}$$

$$\Pi^+(\theta) = \{(t, h) : t\cos(\theta) + h\sin(\theta) \geq C(\theta)\},$$

$$\Pi^-(\theta) = \{(t, h) : t\cos(\theta) + h\sin(\theta) \leq C(\theta)\}.$$

By the definition of $C(\theta)$ it follows that for all $\theta \in [0, 2\pi)$ we have:

$$P[(T, H) \in \Pi^+(\theta)] = P[T\cos(\theta) + H\sin(\theta) > C(\theta)] = P_e$$

In (Huseby et al. 2015a) it was shown that $\mathcal{B}$ may be expressed as:

$$\mathcal{B} = \bigcap_{\theta \in [0, 2\pi)} \Pi^-(\theta),$$

assuming that $\Pi(\theta)$ intersects the boundary of $\mathcal{B}$ for all $\theta \in [0, 2\pi)$. Under this assumption it also follows that:

$$\mathcal{P}(\mathcal{B}) = \{\Pi^+(\theta) : \theta \in [0, 2\pi)\}.$$

We may then use Proposition 2.1 to compute the exceedence probability of $\mathcal{B}$ with respect to $\mathcal{E}$, and get:

$$\begin{aligned} P_e(\mathcal{B}, \mathcal{E}) &= \sup\{P[(T, H) \in \Pi^+] : \Pi^+ \in \mathcal{P}(\mathcal{B})\} \\ &= \sup\{P[(T, H) \in \Pi^+(\theta)] : \theta \in [0, 2\pi)\} \\ &= \sup_{\theta \in [0, 2\pi)} P[T\cos(\theta) + H\sin(\theta) > C(\theta)] = P_e \end{aligned}$$

We then conclude that the contour $\partial\mathcal{B}$ has the correct exceedence probability with respect to $\mathcal{E}$.

Contours constructed this way have the advantage, compared to transformed contours, that it is much easier to argue that the true failure region of a given mechanical construction belongs to the family $\mathcal{E}$. The disadvantage, however, is that one is limited to convex contours. In cases where the joint distribution of (T, H) is concentrated on a non-convex area, a convex contour would typically include significant areas with very little probability mass. In such cases convex contours may lead to overly conservative designs. See (Vanem & Bitner-Gregersen 2015).

3 UPPER BOUND ON THE EXCEEDENCE PROBABILITY

In Subsection 2.1 we explained how to compute the exceedence probability of a convex set by using Proposition 2.1. In this section we approach the problem of computing the exceedence probability of a general environmental contour. More specifically we assume that $\mathcal{B} \subseteq \mathbb{R}^2$ is a *simply connected*, but not necessarily convex set. Intuitively a simply connected set is a connected set with no holes.

As in the previous section we let $\mathcal{E}$ be the family of all convex sets $\mathcal{F} \subseteq \mathbb{R}^2$ such that $\mathcal{F} \cap \mathcal{B} \subseteq \partial\mathcal{B}$. In order to verify that $\partial\mathcal{B}$ has the correct exceedence probability with respect to $\mathcal{E}$, we have to compute $P_e(\mathcal{B}, \mathcal{E})$. Since $\mathcal{B}$ does not need to be convex, we cannot assume that $\mathcal{E}^*$ is equal to $\mathcal{P}(\mathcal{B})$. This problem is illustrated in Figure 1. In this figure the set $\mathcal{B}$ is not convex. Then it is possible to find a set $\mathcal{F} \in \mathcal{E}$ which is not contained in any supporting half-space of $\mathcal{B}$. In fact any half-space containing $\mathcal{F}$ will overlap with the interior of $\mathcal{B}$ and hence cannot be a supporting half-space of $\mathcal{B}$.

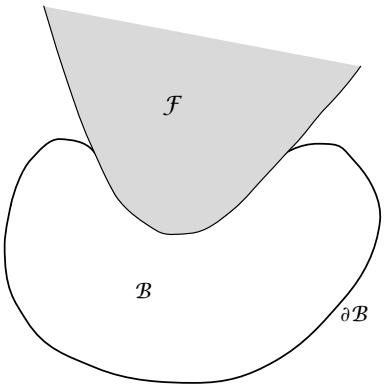

Figure 1: The convex set $\mathcal{F} \in \mathcal{E}$ is *not* contained in any supporting half-space of $\mathcal{B}$.

In order to compute $P_e(\mathcal{B}, \mathcal{E})$ for a general simply connected set we need an efficient way of identifying the family $\mathcal{E}^*$. The fact that $\mathcal{E}^*$ typically is an infinite family makes this difficult

Instead of identifying the family $\mathcal{E}^*$ directly, it can sometimes be easier to introduce an alternative family of failure regions. We denote this family by $\tilde{\mathcal{E}}$, and assume that this family is such that for each $\mathcal{F} \in \mathcal{E}$, there exists a set $\tilde{\mathcal{F}} \in \tilde{\mathcal{E}}$ such that $\mathcal{F} \subseteq \tilde{\mathcal{F}}$. By this assumption we immediately get:

$$P_e(\mathcal{B}, \mathcal{E}) \leq P_e(\mathcal{B}, \tilde{\mathcal{E}}).$$

This means that by introducing the alternative family $\tilde{\mathcal{E}}$ and base the calculations on this, we get an upper bound on the exceedence probability.

The point here is that by choosing $\tilde{\mathcal{E}}$ in a clever way, it may be much easier to compute the upper bound on the exceedence probability.

In order to explain this in more detail, we consider a specific family $\tilde{\mathcal{E}}$. We assume that $\mathcal{B}$ is given, and as before we let $\mathcal{E}$ be the family of all convex sets $\mathcal{F} \subseteq \mathbb{R}^2$ such that $\mathcal{F} \cap \mathcal{B} \subseteq \partial\mathcal{B}$. We then choose an arbitrary convex set $\mathcal{F} \in \mathcal{E}$. Then there exists a maximal set $\mathcal{F}^* \in \mathcal{E}$ such that $\mathcal{F} \subseteq \mathcal{F}^*$ having at least point x_0 in common with the contour $\partial\mathcal{B}$, i.e., $x_0 \in \mathcal{F}^* \cap \partial\mathcal{B}$. We then let $\Pi(x_0)$ be a hyperplane supporting $\mathcal{F}^*$ at x_0, such that $\mathcal{F}^* \subseteq \Pi^+(x_0)$, where $\Pi^+(x_0)$ is the half-space bounded by $\Pi(x_0)$ and containing $\mathcal{F}^*$. Finally, we introduce the set $\tilde{\mathcal{F}}(x_0) = \Pi^+(x_0) \setminus \mathcal{B}_o$. See Figure 2. It is then clear that $\mathcal{F} \subseteq \mathcal{F}^* \subseteq \tilde{\mathcal{F}}(x_0)$. The

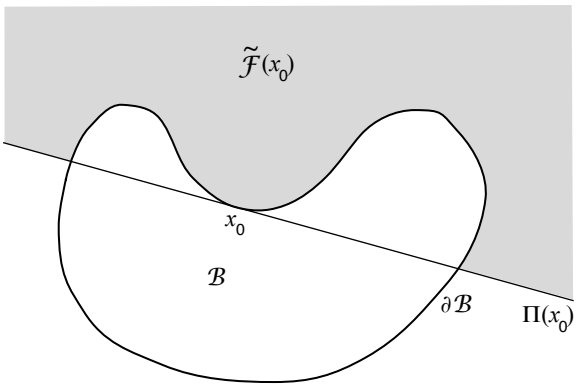

Figure 2: The construction of the set $\tilde{\mathcal{F}}(x_0)$.

same construction can be carried out along the entire border of $\mathcal{B}$. Thus, for any $x \in \partial\mathcal{B}$ we define $\tilde{\mathcal{F}}(x)$ to be the corresponding set constructed as above by identifying a maximal set in $\mathcal{E}$ containing the point x. Moreover, we define $\tilde{\mathcal{E}} = \{\tilde{\mathcal{F}}(x) : x \in \partial B\}$. We then have that for each $\mathcal{F} \in \mathcal{E}$, there exists a set $\tilde{\mathcal{F}} \in \tilde{\mathcal{E}}$ such that $\mathcal{F} \subseteq \tilde{\mathcal{F}}$. We observe that the family $\tilde{\mathcal{E}}$ is indexed by the points in $\partial\mathcal{B}$. Thus, we may estimate $P[(T, H) \in \tilde{\mathcal{F}}(x)]$ for all $x \in \partial\mathcal{B}$ and plot the result. An upper bound on the exceedence probability, $P_e(\mathcal{B}, \mathcal{E})$ can then be found by identifying the maximum value of this function, which by definition is equal to $P_e(\mathcal{B}, \tilde{\mathcal{E}})$.

We also observe that if $\mathcal{B}$ is itself *convex*, we get that $\mathcal{E}^* = \tilde{\mathcal{E}}$. Thus, in this case the upper bound is equal to the exceedence probability of $\mathcal{B}$ with respect to $\mathcal{E}$, i.e., $P_e(\mathcal{B}, \mathcal{E}) = P_e(\mathcal{B}, \tilde{\mathcal{E}})$. On the other hand, if parts of the set $\mathcal{B}$ is strongly non-convex, as in Figure 2 the upper bound can be rather crude.

3.1 *Numerical examples*

In this subsection we illustrate the proposed method by considering two numerical examples introduced in (Vanem & Bitner-Gregersen 2015). More sepcifically, we consider joint long-term models for *significant wave height*, denoted by H, and *wave period* denoted by T. A marginal distribution is fitted to the data for significant wave height and a conditional model, conditioned on the value of significant wave height, is subsequently fitted to the wave period. The joint model is the product of these distribution functions:

$$f_{T,H}(t, h) = f_H(h) f_{T|H}(t|h)$$

Simultaneous distributions have been fitted to data assuming a three-parameter Weibull distribution for the significant wave height, H, and a lognormal conditional distribution for the wave period, T. The three-parameter Weibull distribution is parameterized by a location parameter, γ, a scale parameter α, and a shape parameter β as follows:

$$f_H(h) = \frac{\beta}{\alpha}\left(\frac{h-\gamma}{\alpha}\right)^{\beta-1} e^{-[(h-\gamma)/\alpha]^\beta}, \quad h \geq \gamma.$$

The lognormal distribution has two parameters, the log-mean μ and the log-standard deviation σ and is expressed as:

$$f_{T|H}(t|h) = \frac{1}{t\sqrt{2\pi}} e^{-[(\ln(t)-\mu)^2/(2\sigma^2)]}, \quad t \geq 0,$$

where the dependence between H and T is modelled by letting the parameters μ and σ be expressed in terms of H as follows:

$$\mu = E[\ln(T)|H = h] = a_1 + a_2 h^{a_3},$$

$$\sigma = SD[\ln(T)|H = h] = b_1 + b_2 e^{b_3 h}.$$

The parameters $a_1, a_2, a_3, b_1, b_2, b_3$ are estimated using available data from the relevant geographical location. In the examples considered here the parameters are fitted based on a data set from West Shetland. We consider data for three different cases: *total sea*, *wind sea* and *swell*. The parameters for the three-parameter Weibull distribution are listed in Table 1, while the parameters for the conditional log-normal distribution are listed in Table 2. In all the examples we use a return period of 25 years. The models are fitted using sea states representing periods of 3 hours. Thus, we get 8 data points per 24 hours. Thus, the desired exceedence probability is given by:

$$P_e = \frac{1}{25 \cdot 365.25 \cdot 8} = 1.3689 \cdot 10^{-5}.$$

For more details about these examples we refer to (Vanem & Bitner-Gregersen 2015).

Table 1: Fitted parameter for the three-parameter Weibull distribution for signifcant wave heights

	α	β	γ
Total sea	2.259	1.285	0.701
Wind sea	2.139	1.176	0.318
Swell	2.527	1.460	0.337

Environmental contours for all three cases are constructed using both the traditional approach based on the Rosenblatt transformation, and the alternative approach based on Monte Carlo simulation. In the plots of the environmental contours the x-axis represents the wave period

Table 2: Fitted parameter for the conditional log-normal distribution for wave periods

		$i=1$	$i=2$	$i=3$
Total sea	a_i	1.069	0.898	0.243
	b_i	0.025	0.263	-0.148
Wind sea	a_i	0.005	1.694	0.186
	b_i	0.050	0.191	-1.074
Swell	a_i	1.069	0.898	0.243
	b_i	0.025	0.263	-0.148

measured in seconds (i.e., T), while the y-axis represents the significant wave heights measured in meter (i.e., H).

In the plots of $P[(T,H) \in \tilde{\mathcal{F}}(x)]$ as a function of the point $x \in \partial\mathcal{B}$, we let the point x run counterclockwise along the Rosenblatt contour. The starting point is marked by a small blue circle in the contour plots. A total of 360 points are used in each of these plots. The x-axis in these plots represents the index of these points.

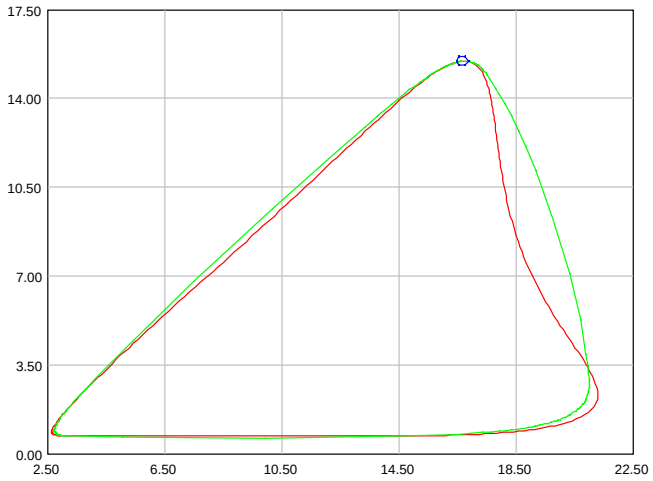

Figure 3: Environmental contours for *total sea* constructed using the Rosenblatt transformation (red curve) and using Monte Carlo simulation (green curve). The small blue circle marks the starting point of the Rosenblatt contour.

The environmental contours for the *total sea* case are shown in Figure 3. The corresponding plot of the upper bound on the exceedence probability, $P[(T,H) \in \tilde{\mathcal{F}}(x)]$ as a function of the point $x \in \partial\mathcal{B}$ for the Rosenblatt contour is shown in Figure 4. The largest value of $P[(T,H) \in \tilde{\mathcal{F}}(x)]$ is $5.1498 \cdot 10^{-5}$ which occurs when $x = (20.4169, 4.3679)$. Thus, the upper bound on the exceedence probability is almost four times greater than the desired value. By examining the plot, we observe that there are points where the curve is below the desired value value as well. However, even the average value of the curve is obviously greater than the desired exceedence probability. Typically, the points where curve is above the desired value corresponds to points on the Rosenblatt contour which are inside the Monte Carlo contour, while the points where curve is below the desired value corresponds to points on the Rosenblatt contour which are outside the Monte Carlo contour.

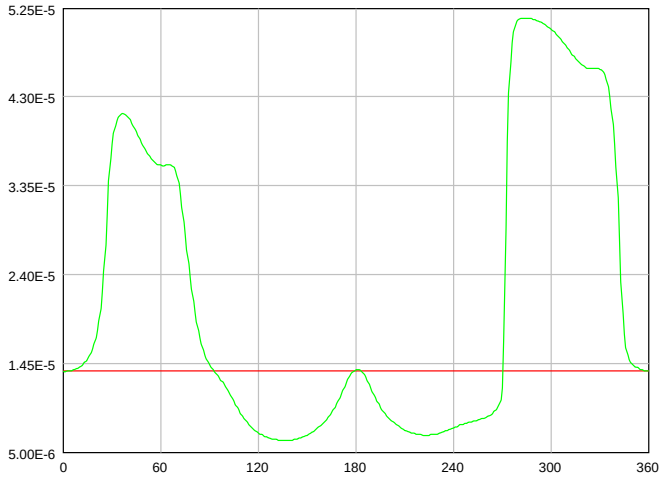

Figure 4: $P[(T,H) \in \tilde{\mathcal{F}}(x)]$ as a function of the point $x \in \partial\mathcal{B}$ for *total sea* for the Rosenblatt contour (green curve). The red curve represents the desired exceedence probability $P_e = 1.3689 \cdot 10^{-5}$.

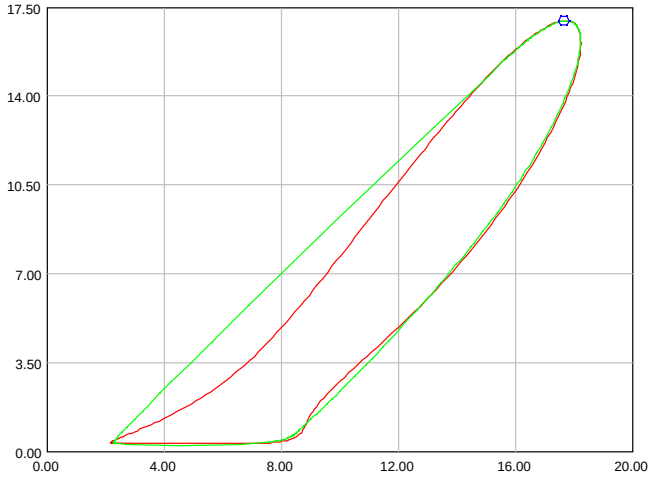

Figure 5: Environmental contours for *wind sea* constructed using the Rosenblatt transformation (red curve) and using Monte Carlo simulation (green curve). The small blue circle marks the starting point of the Rosenblatt contour.

The environmental contours for the *wind sea* case are shown in Figure 5. The corresponding plot of the upper bound on the exceedence probability, $P[(T,H) \in \tilde{\mathcal{F}}(x)]$ as a function of the point $x \in \partial\mathcal{B}$ for the Rosenblatt contour is shown in Figure 6. The largest value of $P[(T,H) \in \tilde{\mathcal{F}}(x)]$ is $8.6864 \cdot 10^{-5}$ which occurs when $x = (5.7685, 2.5097)$. Thus, the upper bound on the exceedence probability is more than six times greater than the desired value.

Finally, the environmental contours for the *swell* case are shown in Figure 7. The corresponding plot of the upper bound on the exceedence probability, $P[(T,H) \in \tilde{\mathcal{F}}(x)]$ as a function of the point $x \in \partial\mathcal{B}$ for the Rosenblatt contour is shown in Figure 8. The largest value of $P[(T,H) \in \tilde{\mathcal{F}}(x)]$ is $4.7114 \cdot 10^{-5}$ which occurs when $x = (20.3569, 4.3639)$. Thus, the upper bound on the exceedence probability is about three and half times greater

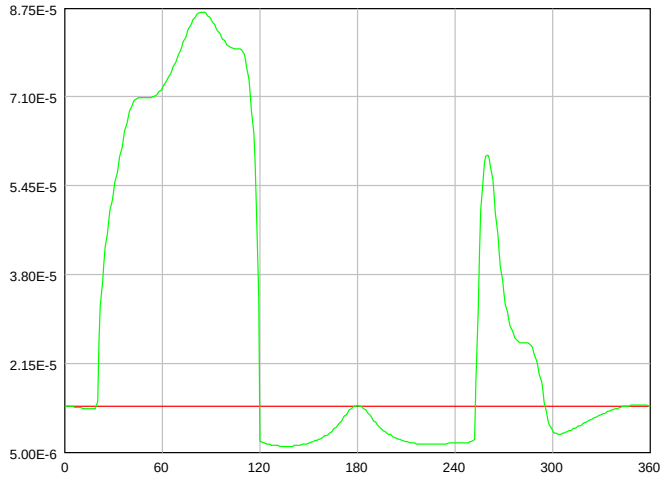

Figure 6: $P[(T,H) \in \tilde{\mathcal{F}}(x)]$ as a function of the point $x \in \partial\mathcal{B}$ for *wind sea* for the Rosenblatt contour (green curve). The red curve represents the desired exceedence probability $P_e = 1.3689 \cdot 10^{-5}$.

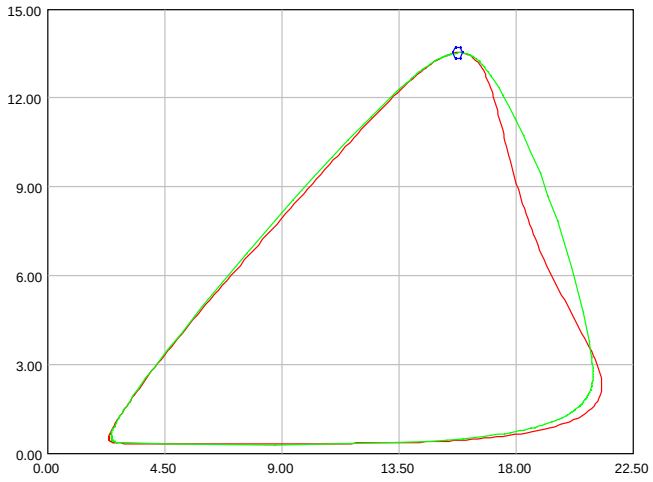

Figure 7: Environmental contours for *swell* constructed using the Rosenblatt transformation (red curve) and using Monte Carlo simulation (green curve). The small blue circle marks the starting point of the Rosenblatt contour.

than the desired value.

Summarizing all the results from these three examples we see that the true value of the exceedence probability of the environmental contour obtained using the Rosenblatt transformation appears to be much larger than the desired value. We also observe that the value of $P[(T,H) \in \tilde{\mathcal{F}}(x)]$ varies a lot as the point x is moved along the contour. This indicates that a design based on this contour may not have the desired failure probability. In fact, depending on the chosen design point, the failure probability may be considerably greater than the desired value, but it may also be lower than this value. In contrast an environmental contour obtained using the Monte Carlo simulation approach will always have the desired exceedence probability. Thus, in cases where the true failure region is convex, a design based on this contour will have a failure probability which is less than or equal to the desired exceedence probability.

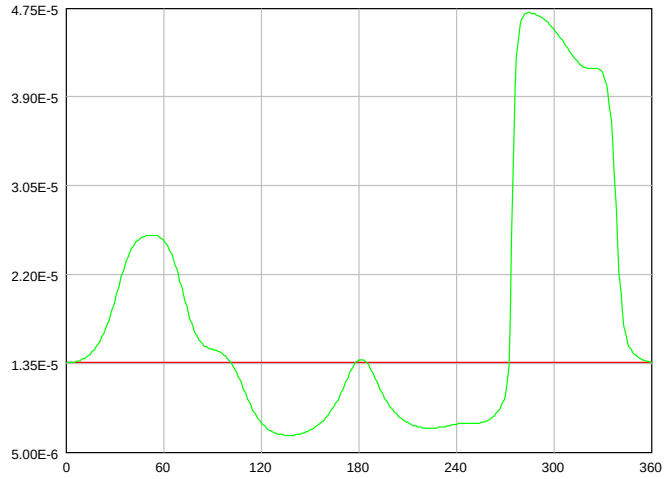

Figure 8: $P[(T,H) \in \tilde{\mathcal{F}}(x)]$ as a function of the point $x \in \partial\mathcal{B}$ for *swell* for the Rosenblatt contour (green curve). The red curve represents the desired exceedence probability $P_e = 1.3689 \cdot 10^{-5}$.

While the results for the environmental contours obtained using the Rosenblatt transformation are unsatisfactory, we should keep in mind that since these contours are clearly not convex, the upper bound can be crude. In the next section we shall investigate this further.

4 LOCALLY CONCAVE SEGMENTS

We recall from the examples considered in the previous section, that the probability $P[(T,H) \in \tilde{\mathcal{F}}(x)]$ typically had its highest values whenever the point x was located in a part of the contour which was strongly non-convex. In this section we would like to derive a method for identifying a maximal convex failure region which covers such a part. In order to do so, we parametrize the contour ∂B. That is, we assume that we have found functions g_t og g_h and an interval $\Omega \subseteq \mathbb{R}$ such that:

$$\partial\mathcal{B} = \{(t,h) = (g_t(s), g_h(s)) : s \in \Omega\}.$$

Intuitively, this means that when the parameter s runs through the interval Ω, then the point $(g_t(s), g_h(s))$ runs through $\partial\mathcal{B}$. As a convention we always choose the parametrization so that each of the points in $\partial\mathcal{B}$ occurs exactly once as s runs through Ω, and such that the point $(g_t(s), g_h(s))$ runs through $\partial\mathcal{B}$ counterclockwise as s runs through Ω from the lowest to the highest value.

We now define the concepts of *local convexity* and *local concavity* for the contour $\partial\mathcal{B}$ as follows. We say that $\partial\mathcal{B}$ is *locally convex* at the point $(t,h) = (g_t(s), g_h(s))$, where $s \in \Omega$, if there exists an open interval $\Omega_s \subseteq \Omega$ where $s \in \Omega_s$, such that for all $s_1, s_2 \in \Omega_s$ the line segment between the points $(g_t(s_1), g_h(s_1))$ and $(g_t(s_2), g_h(s_2))$ is entirely contained in $\mathcal{B}$. Similarly, we say that $\partial\mathcal{B}$ is *locally concave* in the point $(t,h) = (g_t(s), g_h(s))$, where $s \in \Omega$, if there exists an open interval $\Omega_s \subseteq \Omega$ where $s \in \Omega_s$, such that for all $s_1, s_2 \in \Omega_s$ the line segment between the points $(g_t(s_1), g_h(s_1))$ and $(g_t(s_2), g_h(s_2))$ is entirely (except for the end points) contained in the complement of $\mathcal{B}$. Note

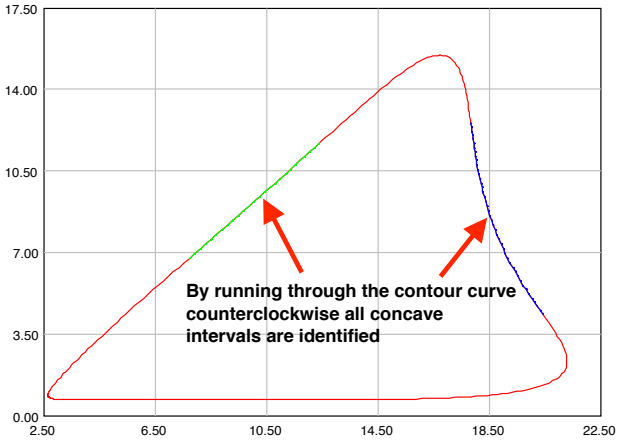

Figure 9: Identifying intervals of points where $\partial\mathcal{B}$ is locally concave

that if $\mathcal{B}$ is locally convex at a point (t, h), then the complement of $\mathcal{B}$ is locally concave at the same point. Similarly, if $\mathcal{B}$ is locally concave at a point (t, h), then the complement of $\mathcal{B}$ is locally convex at the same point.

If we travel along the set $\partial\mathcal{B}$ counterclockwise, local convexity corresponds to *left turns*, while local concavity corresponds to *right turns*. By using this interpretation it is easy to construct an algorithm for identifying intervals of points where $\partial\mathcal{B}$ is locally concave. See Figure 9.

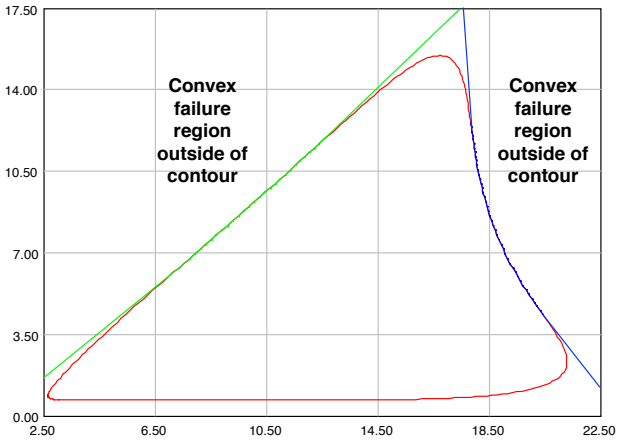

Figure 10: Maximal convex failure regions constructed from locally concave intervals.

Having identified these intervals we use the fact that the complement of $\mathcal{B}$ is locally convex in the same intervals. Thus, we can construct maximal convex failure regions by extending these intervals of $\partial\mathcal{B}$ by straight lines, and let these maximal failure regions be the area separated from $\mathcal{B}$ by the resulting lines. See Figure 10. Since $\mathcal{B}$ typically has a smooth boundary, there will only be a finite number of such maximal convex failure regions. It is then easy to estimate the failure probabilities associated with these maximal failure regions using Monte Carlo simulation. The exceedence probability can then be estimated by taking the maximum of these estimated probabilities.

4.1 *Numerical examples*

In this subsection we proceed with the three examples introduced in Subsection 3.1, and compute the exceedence probability by identifying the intervals of points where $\partial\mathcal{B}$ is locally concave. We then construct maximal convex failure regions by extending these parts of $\partial\mathcal{B}$ by straight lines as shown in Figure 10. The resulting estimated exceedence probabilities are listed in Table 3.

Table 3: Estimated exceedence probabilities for the environmental contours obtained using the Rosenblatt transformation

	$P_e(\mathcal{B}, \mathcal{E})$
Total sea	$3.7327 \cdot 10^{-5}$
Wind sea	$3.8988 \cdot 10^{-5}$
Swell	$3.6190 \cdot 10^{-5}$

We observe that these probabilities are much smaller than the crude upper bounds obtained by considering the maximum of $P[(T, H) \in \tilde{\mathcal{F}}(x)]$. Still for all three cases the estimated exceedence probabilities are more than twice the desired value, $1.3689 \cdot 10^{-5}$. Thus, while the environmental contours obtained using the Rosenblatt transformation typically fits the joint distribution of the environmental variable better than the contours obtained using the Monte Carlo simulation approach, the resulting exceedence probability, as defined in this paper, may be considerably larger than desired.

5 CONCLUSIONS

In the present paper we have introduced a precise definition of the exceedence probability of a given environmental contour with respect to a family of failure regions. We believe that this concept is needed in order to evaluate the probabilistic properties of a given contour. Throughout the numerical examples we have seen that the traditional approach based on the Rosenblatt transformation can produce a contour with an exceedence probability which is higher than desired. The alternative approach based on Monte Carlo simulation, however, is constructed so that the exceedence probability is always correct. On the other hand the contour based on Monte Carlo simulation can sometimes be too conservative and include areas with very low probability when the joint distribution of the environmental variables are concentrated in a non-convex region. In an upcoming paper we will show how to modify the contour based on Rosenblatt transformation so that the exceedence probability becomes correct. This makes it possible to obtain contours that fit the main parts of the joint distribution better while keeping the exceedence probability under control. It should be mentioned though that the resulting contour can sometimes be overly conservative in some areas. Still, by comparing different contours with the same exceedence probability makes it easier to choose the best one for the given application.

ACKNOWLEDGEMENTS

This paper has been written with support from the Research Council of Norway (RCN) through the project *ECSADES* En-

vironmental Contours for Safe Design of Ships and other marine structures.

REFERENCES

Baarholm, G.S., Haver, S. and Økland, O.D. Combining contours of significant wave height and peak period with platform response distributions for predicting design response. *Marine Structures* (23): 147–163, 2010.

Ditlevsen, O. Stochastic model for joint wave and wind loads on offshore structures. *Structural Safety* (24): 139–163, 2002.

Fontaine, E., Orsero, P., Ledoux, A., Nerzic, R., Prevesto, M. and Quiniou, V. Reliability analysis and response based design of a moored FPSO in West Africa. *Structural Safety* (41): 82–96, 2013.

Haver, S. On the joint distribution of heights and periods of sea waves. *Ocean Engineering* (14): 359–376, 1987.

Haver, S. and Winterstein, S. Environmental contour lines: A method for estimating long term extremes by a short term analysis. *Transactions of the Society of Naval Architects and Marine Engineers* (116): 116–127, 2009.

Huseby, A. B., Vanem, E., Natvig, B. A new approach to environmental contours for ocean engineering applications based on direct Monte Carlo simulations. *Ocean Engineering*, (60): 124–135, 2013.

Huseby, A. B., Vanem, E., Natvig, B. Alternative environmental contours for structural reliability analysis. *Structural Safety*, (54): 32–45, 2015.

Huseby, A. B., Vanem, E., Natvig, B. A new Monte Carlo method for environmental contour estimation, In *Safety and Reliability : Methodology and Applications*, Proceedings of the European safety and reliability Conference, Taylor & Francis. ISBN 978-1-138-02681-0. Chapter 270. 2091–2098, 2015.

Jonathan, P., Ewans, K. and Flynn, J. On the estimation of ocean engineering design contours. In: *Proc. 30th International Conference on Offshore Mechanics and Arctic Engineering (OMAE 2011)* American Society of Mechanical Engineers (ASME), 2011.

Moan, T. Development of accidental collapse limit state criteria for offshore structures. *Structural Safety* (31): 124–135, 2009.

Rosenblatt, M. Remarks on a Multivariate Transformation. *The Annals of Mathematical Statistics* (23): No 3, 470–472, 1952.

Vanem, E. and Bitner-Gregersen, E. Stochastic modelling of long-term trends in wave climate and its potential impact on ship structural loads. *Applied Ocean Research*, (37): 235–248, 2012.

Vanem, E. and Bitner-Gregersen, E. Alternative Environmental Contours for Marine Structural Design – A Comparison Study. *Journal of Offshore Mechanics and Arctic Engineering*, (137): 051601-1–051601-8, 2015.

Winterstein, S., Ude, T., Cornell, C., Bjerager, P. and Haver, S. Environmental parameters for extreme response: Inverse FORM with omission factors. In: *Proc. 6th International Conference on Structural Safety and Reliability*, 1993.